J Fluoresc (2015) 25:663–673
DOI 10.1007/s10895-015-1552-y

ORIGINAL PAPER

Novel Multicolor Schiff Base Polymers Prepared via Oxidative Polycondensation

İsmet Kaya · Esra Kılavuz

Received: 26 September 2014 / Accepted: 5 March 2015 / Published online: 14 March 2015

Abstract A series of diimine Schiff bases and their polymers were synthesized via the oxidative polycondensation reaction. The structures of the compounds were confirmed by ^{1}H-NMR, ^{13}C-NMR, FT-IR and UV–vis spectral measurements. Electrochemical and optical band gap values of synthesized compounds were determined by cyclic voltammetry (CV) and UV–vis measurements, respectively. Fluorescence measurements of the compounds were conducted in various solvents. The effects of solution concentration on the fluorescence spectra were investigated and quantum yield was calculated for the polymer of 5-(diethylamino)-2-(biphenylmethylene) hydrazonomethylphenol (PDEAHP). According to fluorescence measurements, the quantum yield of PDEAHP was found as 16 % in DMF solution. Thermal characteristics of polymers were studied by TG-DTA and DSC analyses.

Keywords Fluorescence · Concentration effects · Quantum yield · Oxidative polymerization

Introduction

In recent years, the various functional polymers have been obtained by chemical oxidative polymerization [1]. Poly(azomethines) (PAMs), are classes of conjugated polymers containing nitrogen atoms in a polymer backbone [2]. PAMs and their oligophenol derivates have been widely investigated in respect of their optical, electrochemical, thermal and conductivity measurements [3–5]. Coupling mechanism of the Schiff base substituted phenol monomers have been also studied and two coupling mechanisms are suggested: C-O and C-C couplings [6–9]. The effect of the coupling rate on thermal stability has been investigated and it is found that increasing C-O coupling rate also decrease the thermal stability of the oligophenol. Poly(azomethine-urethane); (E)-4-((2 hydroxyphenylimino) methyl)-2-methoxyphenyl 6-acetamidohexylcarbamate (HDI-*co*-3-DHB-2-AP) was synthesized as in the literature from Kaya et al. and it was used as a new fluorescent probe for detection of Cd(II) concentration [10]. The HDI-*co*-3-DHB-2-AP sensor was prepared as in the literature [11] and determined as good candidate for optical detection of Cd(II) ion. According to Kaya et al., the most important advantage of the proposed Cd(II) sensor is easy production with fine sensing and stable properties. Selectivity study of the new Cd(II) sensor was investigated and a considerable selectivity was obtained according to relative intensity change values [10].

In this study, new polyphenol derivates were synthesized via oxidative polycondensation reaction. The structures and characterizations of compounds were made by Fourier transform infrared spectroscopy (FT-IR), Ultraviolet–visible spectroscopy (UV–vis), Nuclear Magnetic Resonance Spectroscopy (NMR), cyclic voltammetry (CV), PL, TG-DTA, DSC and SEC measurements. Emission characteristics of resulting products were determined from fluorescence measurements. We also, reported the effect of concentrations on the both intensity and wavelength of the emission spectra. It was understood that PDEAHP exhibited the different emission colors depending on the changing concentrations. On the other hand, PHB showed white fluorescence emission.

Materials and Methods

Materials

Benzophenonehydrazone (BPH), 4-diethylaminosalicylaldehyde (DASA), 3-hiydroxy-4-methoxybenzaldehyde (HMBA) were

İ. Kaya (✉) · E. Kılavuz
Faculty of Science and Arts, Department of Chemistry, Polymer Synthesis and Analysis Lab, Çanakkale Onsekiz Mart University, 17020 Çanakkale, Turkey
e-mail: kayaismet@hotmail.com

supplied from Alfa Easer and 2,4-dihydroxybenzaldehyde (DHBA), 2-hydroxy-1-naphtaldehyde (HNA) and salicylaldehyde (SA) were supplied from Across Organics, Fluka and Merck companies (Germany), respectively. Sodium hypochlorite (NaOCl) (30 % aqueous solution) was provided from Paksoy Chem. Co. (Turkey).

Synthesis of Schiff Bases

Schiff bases abbreviated as 2-(((diphenylmethylene)hydrazono)methyl)phenol (HB), 4-(((diphenylmethylene)hydrazono)methyl)benzene-1,3-diol(HBD), 5-(((diphenylmethylene)hydrazono)methyl)-2-methoxyphenol (HMP), 5-(diethylamino)-2-(biphenylmethylene)hydrazonomethylphenol(DEAHP), 3(((diphenylmethylene)hydrazono) methyl)naphthalene-2-ol (HN) were synthesized by the condensation reaction of benzophenonehydrazone (BPH) with 4-diethylamino salicylaldehyde, 3-hydroxy-4-methoxybenzaldehyde, 2,4-dihydroxybenzaldehyde, 2-hydroxy-1-naphtaldehyde and salicylaldehyde, respectively. The Synthesis reactions were performed as follows Scheme 1. BPH (1.5 g 0.008 mol) was placed into a 250 mL three-necked round-bottom flask which was fitted with condenser, thermometer and magnetic stirrer. Fifty milliliters of methanol was added into the flask and reaction mixture was heated up to 60 °C. A solution of equivalent mol of aldehydes (0.01 mol) in 20 mL methanol was added into the flask. Reaction was maintained for 5 h under reflux [12]. The yields of HB, HBD, HMP, DEAHP and HN were found as 88, 91, 89, 90 and 92 %, respectively.

Synthesis of the Polyphenols Containing Imine Bonding

The synthesized monomers (HBD, HB) were converted into their polymer derivatives through oxidative polycondensation reactions in an aqueous alkaline medium using NaOCl (30 %) as the oxidant, as in the literature [13]. PHMP, PDEAHP, PHN were synthesized via oxidative polycondensation of HMP, DEAHP and HN in an aqueous solution (30 %) acetic acid at 60 °C (Scheme 2). Then, a solution of NaOCl (30 %) was added into the mixture drop by drop for 2 h [14].

Characterization Techniques

The solubility tests were done in an ultrasonic bath by using 1 mg sample and 1 mL solvent at room temperature. The infrared and ultraviolet–visible spectra of compounds were measured by Perkin Elmer FT-IR Spectrum and Analytikjena Specord 210 Plus, respectively. The FT-IR spectra were recorded using universal ATR sampling accessory (4000–

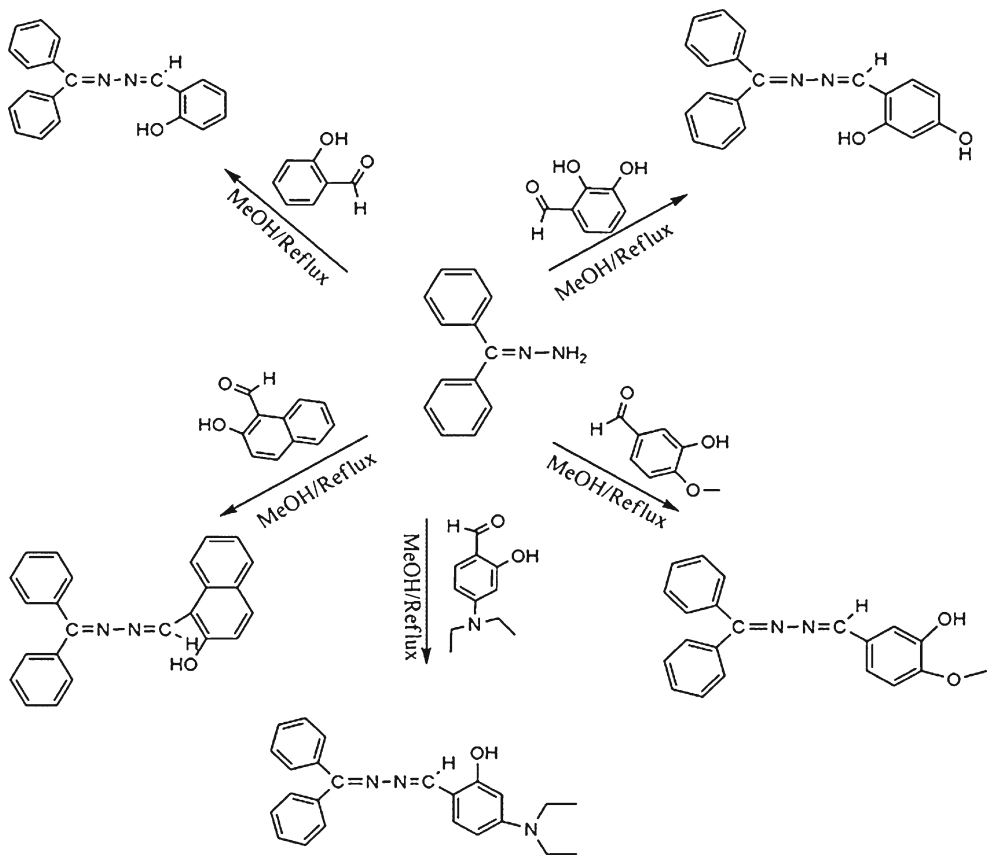

Scheme 1 Synthesis reactions of Schiff bases

Scheme 2 Synthesis reactions of polymers

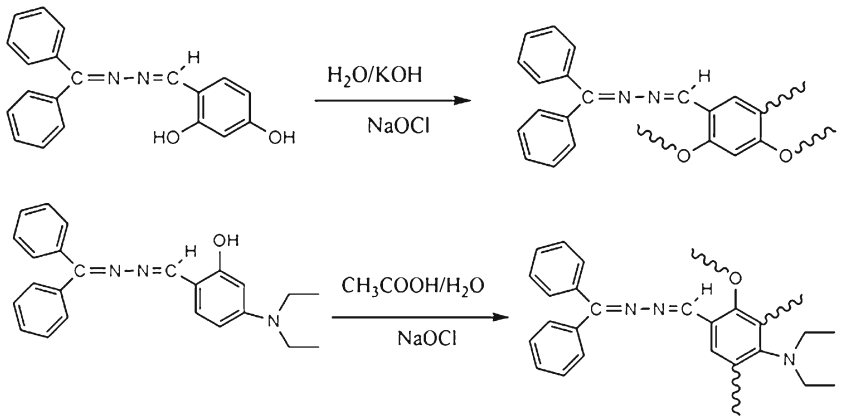

650 cm^{-1}). ^{1}H and ^{13}C-NMR spectra (Bruker AC FT-NMR spectrometer operating at 400 and 100.6 MHz, respectively) were recorded by using DMSO-d_6 as a solvent at 25 °C. Tetramethylsilane was used as internal standard. DSC measurements were performed between 20 and 450 °C (in N_2, rate 10 °C/min) using a Perkin Elmer Pyris Sapphire DSC instrument. The average molecular weight (Mn), average molecular weight (Mw) and polydispersity index (PDI) were determined by size exclusion chromatography (SEC) techniques of Shimadzu Co. For SEC investigations a SGX (100 Å and 7 nm diameter loading material) 3.3 mm i.d. × 300 mm column was used eluent: DMF/Methanol (0.4 mL/min, v/v, 1/4), polystyrene standards. Refractive index detector (RID) was used to analyze the products at 25 °C. Cyclic voltammetry (CV) measurements were carried out with a CHI 660 C Electrochemical Analyzer (CH Instruments, Texas, USA). All the experiments were performed in a dry box filled with argon at room temperature. Glassy carbon working electrode (GCE), Ag wire as reference electrode, and platinum wire as counter electrode were used. A Shimadzu RF-5301PC spectrofluorophotometer was used for fluorescence measurements [14]. The surface morphologies of polymers were monitored by using a JEOL JSM-7100F Schottky field emission scanning electron microscope.

Results and Discussion

Structural Characterization of the Synthesized Compounds

Oxidative polycondensation reaction of Schiff bases monomers were conducted in alkaline medium and NaOCl was used as oxidant. The general reaction procedures are given in Scheme 2. The structures of the monomer and polymer were identified by FT-IR, UV–vis and NMR analyses. The FT-IR spectral data were given in Table 1. As seen in Table 1, monomers and corresponding polymers showed similar absorption characteristics. Schiff bases containing hydroxyl groups at the *ortho* position were not observed hydroxyl stretching due to intermolecular hydrogen interaction. The formation of Schiff base monomers were confirmed by presence the imine (HC=N) vibrations in the spectra. However, the weak C=O stretching peak (1650s cm^{1}) was observed due to formation of a keto-amine form. Aliphatic C-H stretching

Table 1 FT-IR data of compounds

	Functional Groups (cm^{-1})					
Compounds	Ar-C-H	O-H	C-H (imine)	-C=N	Ar-C=C	Alipht.-C-H
HB	3056	–	2975–2993	1605	1570–1543	–
PHB	3055	–	3025	1573	1570–1486	–
HBD	3022	3511	2970–2990	1606	1590–1521	–
PHBD	3056	–	–	1594	1575–1490	–
HMP	3010	3305	3097–3107	1605	1577–1504	–
PHMP	3056	3397	–	1597	1590–1490	–
DEAHP	3057	–	3041–3050	1619–1588	1597–1576	
PDEAHP	3058	–	–	1594	1556–1468	2970–2871
HN	3020	–	2987–3015	1587	1588–1570	–
PHN	3056	–	–	1571	1514–1468	–

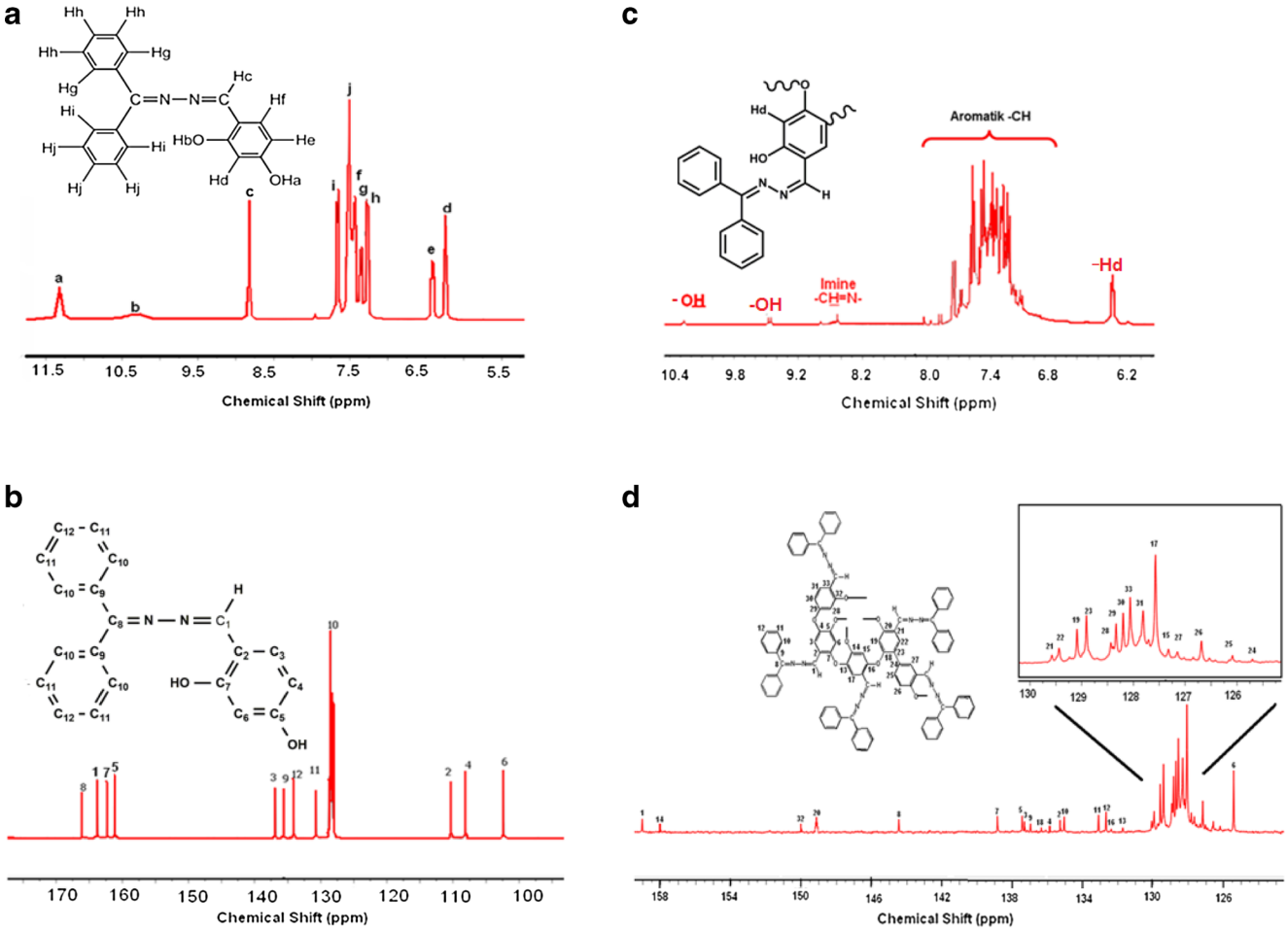

Fig. 1 ^{1}H-NMR and ^{13}C-NMR spectra of HBD (**a**, **b**) and PHBD (**c**, **d**)

Table 2 ^{1}H-NMR and ^{13}C-NMR data of compounds

Compounds	Spectral data (δ ppm)
HB	^{1}H-NMR (DMSO$_{-d6}$): 8.97 (s, -OH), 7.69 (s, -CH=N-), 7.70 (d, -H$_f$), 7.55 (t, -H$_j$), 7.51(t,-H$_g$) 6.92 (t, -H$_c$), 6.91 (t, -H$_b$), 6.83 (d, -H$_a$).
PHB	^{1}H-NMR (DMSO$_{-d6}$): 11.20–10.95 (s, -OH), 8.96–9.09 (s, -CH=N-), 6.96–7.78 (m, aromatic protons).
HBD	^{1}H-NMR (DMSO$_{-d6}$): 11.32 (s, -OH$_a$), 10.32 (s, -OH$_b$) 8.82 (s, -CHc=N-), 7.66 (d, -H$_f$), 7.47 (t,-H$_g$), 7.43 (d, -H$_h$), 7.36 (t, -H$_j$), 6.6 (d,-He), 6.40 (s, -H$_d$).
PHBD	^{1}H-NMR (DMSO$_{-d6}$): 10.26 (s, -OH), 9.2 (d, -OH), 8.5 (s, -CH=N-), 6.70–8.03 (m, aromatic protons), 6.30 (s, -H$_d$).
HBD	^{13}C-NMR (DMSO$_{-d6}$): 166.13 (C8-ipso), 163 (C1), 162.36 (C7-OH), 161.12(C5-OH), 136.28 (C3), 136.79 (C9-ipso), 135.6 (C12), 128.48 (C11), 110 (C2-ipso), 108 (C4), 102.35 (C6).
PHBD	^{13}C-NMR (DMSO$_{-d6}$):159.04 (C1H=N), 144.4 (C8=N), 125.43–144.40 (aromatic carbons).
HMP	^{1}H-NMR (DMSO$_{-d6}$): 9.79(s,-OH), 9.3(s,-CH=N-), 7.64 (d, -H$_f$), 7.48 (t, -H$_g$), 7.28 (d, -H$_h$), 7.29 (t, -H$_j$), 8.47 (s, -Ha), 7.10 (d, -H$_b$), 6.98 (d, -H$_c$), 3.33 (s, -OCH$_3$).
PHMP	^{1}H-NMR (DMSO$_{-d6}$):10.29 (s,-OH$_1$), 7.96(s, -CH=N-), 6.78–7.74 (m, aromatic protons), 2.52 (s, -OCH$_3$).
DEAHP	^{1}H-NMR (DMSO$_{-d6}$):11.31 (s, -OH), 8.72(s, -CH=N-), 7.66 (d, -H$_f$), 7.64(t,-H$_g$), 7.53 (d, -H$_h$), 7.51 (t, -H$_j$), 7.25 (s, -Ha),7.29 (d, -H$_b$), 6.26 (s, -H$_c$), 3.34 (m, -CH$_2$), 1.08 (t, -CH$_3$).
PDEAHP	^{1}H-NMR (DMSO$_{-d6}$): 11.5 (s,-OH), 9.62 (s, -CH=N-), 8.91 (s, -H$_b$), 8.79 (s, -Ha), 6.31 (s, -Hc), 7.25–7.95 (m, aromatic protons) 3.14 (m, -CH$_2$), 1.11 (t, -CH$_3$).
HN	^{1}H-NMR (DMSO$_{-d6}$):12.71(s,-OH), 9.82 (s,-CH=N-), 7.58 (d, -H$_f$), 7.51(t,-H$_g$), 7.41 (d, -H$_h$), 7.10 (t, -H$_j$), 8.45 (d,-Ha),7.96(d, -H$_b$), 7.86 (d, -H$_c$), 7.74 (d, -H$_d$), 7.35(t, -H$_e$).
PHN	^{1}H-NMR (DMSO$_{-d6}$):12.71 (s, -OH), 9.83 (s, -CH=N-), 8.44 (d,-Ha), 7.96 (d, -H$_b$), 7.86 (d, -H$_c$), 7.77 (d, -H$_d$), 7.57–7.08 (m, aromatic protons).

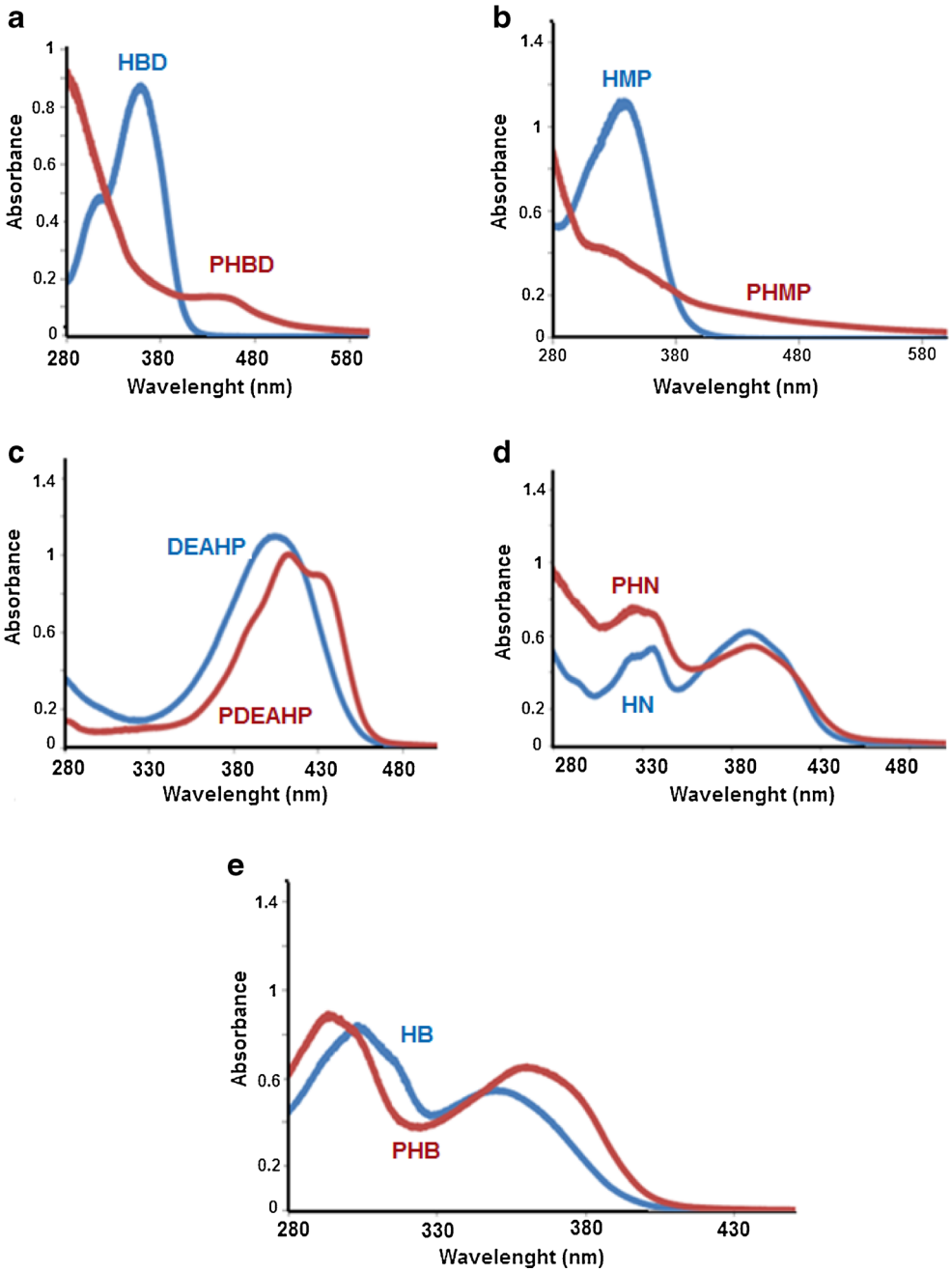

Fig. 2 UV–vis spectra of HBD/PHBD (**a**), HMP/PHMP (**b**), DEAHP/PDEAHP (**c**), HN/PHN (**d**), HB/PHB (**e**)

vibrations of methyl (-CH_3) groups were observed at 2970–2871 cm^{-1}. Polymers exhibited expanded peaks due to their polyconjugated the structures.

^{1}H-NMR and ^{13}C-NMR spectra of the synthesized HBD and PHBD are shown in Fig. 1. The phenolic, azomethine and aromatic proton signals were appeared at 11.32, 10.32, 8.94, 7.67, 6.23 ppm, respectively. ^{13}C-NMR spectrum of HBD indicated that the multiples in 136–102 ppm. 161.21, 162.16, 163.71, 166 ppm were attributed to aromatic carbon signals due to C_5-OH, C_7-OH HC_1-N and C_8=N carbon signals, respectively. FT-IR and NMR analyses confirmed the proposed monomer structure. ^{13}C-NMR and ^{1}H-NMR spectra of PHBD showed that the polymerization occurred via C4 carbon and the phenolic O-H position. The broad signals observed between from 8.0 to 6.26 ppm were attributed to phenylene protons with the different chemical surroundings. The presence of low proton signal (Ha) assigned that the polymerization occurred via Hb elimination. Due to a long distance interaction between $\underline{H}_f$ and N=C-$\underline{H}$a doublet pick at 9.5 ppm was observed in Fig. 1. The NMR analyses data of the synthesized compounds are summarized in Table 2.

According to the proton integration value etheric bond densities of polymers changed the following order: PDEAHP=PHN<PHB<PHBD<PHMP.

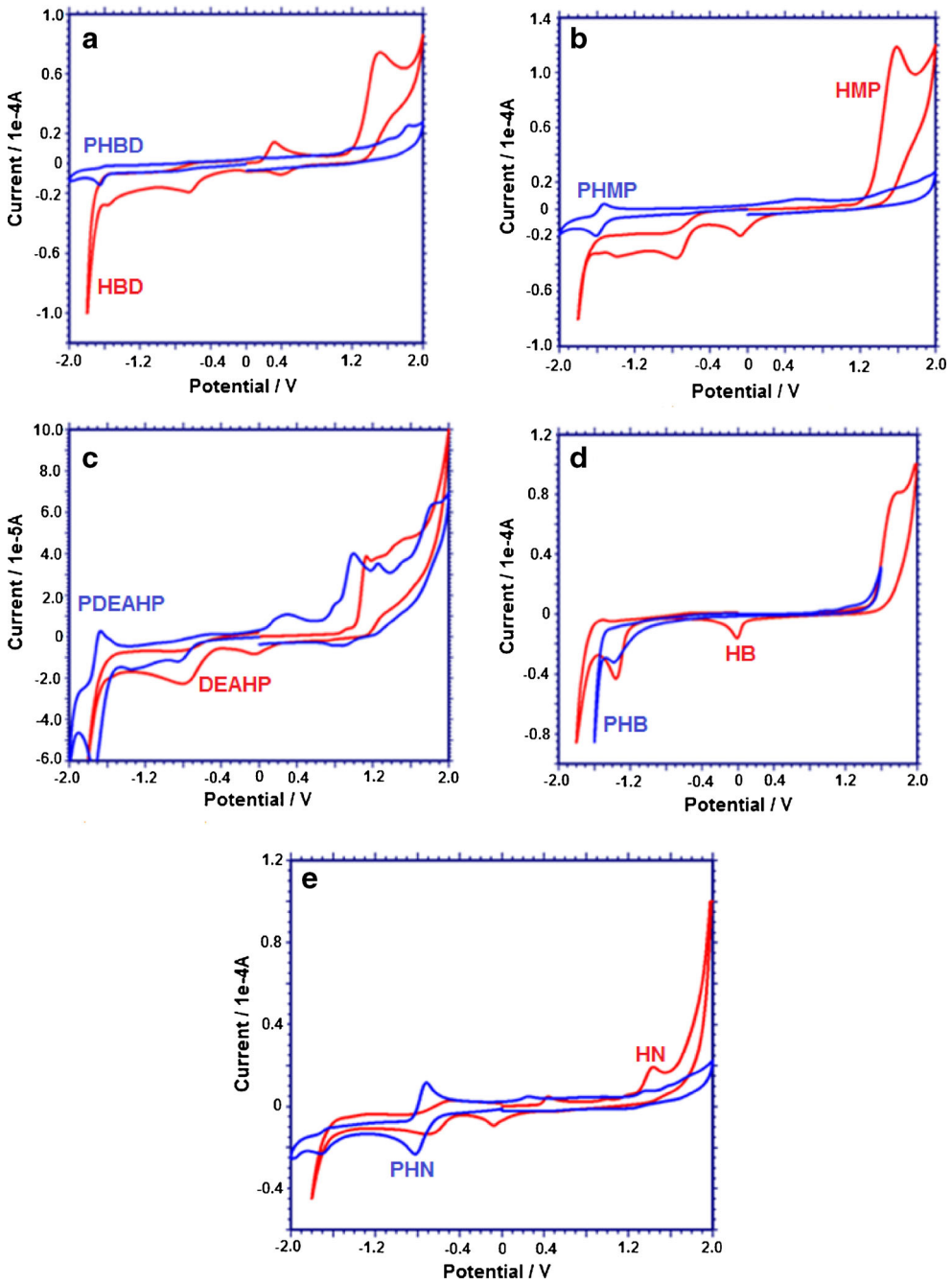

Fig. 3 CV voltammograms of HBD/PHBD (**a**), HMP/PHMP (**b**), DEAHP/PDEAHP (**c**), HB/PHB (**d**), HN/PHN (**e**)

Optical and Electrochemical Properties

The UV–vis spectra of the synthesized compounds are shown in Fig. 2. UV–vis spectra of all synthesized compounds were recorded in DMF at 25 °C. It was understood that, R band ($n \rightarrow \pi^*$ electronic transition) for polymers was broadened. This shift to the red wavelength was attributed to the presence of different-sized polymer chains. Optical band gap values (E_g) are determined as in the literature [15]:

$$E_g = 1242/\lambda_{onset} \quad (1)$$

The calculated optical band gaps had lower than corresponding Schiff base monomers. This case was attributed to

Table 3 The electrochemical (E_g') and optical (E_g) band gaps values of synthesized compounds

	DEAHP	PDEAHP	HBD	PHBD	HMP	PHMP	HB	PHB	HN	PHN
Eg′ (eV)	2.77	1.30	2.98	2.86	2.20	2.12	3.11	2.50	2.30	2.20
Eg (eV)	2.70	2.60	3.00	2.90	2.42	2.26	3.07	3.03	2.80	2.73

due to the polyconjugated structures of polymers. The optical band gaps of polymers changed the following order: PDEA HP<PHMP<PHN<PHB<PHBD.

As shown, PDEAHP has the smallest optical band gap value. It owes to amine functional group (-NEt_2) which is mesomeric electron releasing. The optical band gap value of PHMP is the bigger than PDEAHP, because methoxy group on PHMP is mesomeric electron releasing however it is inductive electron-withdrawing group. Aromatic naphthalene ring has provided electron conjugation to PHN. As results, the structures of PHB and PHBD compounds were similar as electron band gaps.

The cyclic voltammograms of the synthesized compounds were recorded using platinum working electrode, Ag wire as the reference electrode, and platinum wire as the counter electrode in acetonitrile/DMSO solvent mixtures. The CV voltammograms of all compounds are given in Fig. 3. According to the cyclic voltammetry (CV) measurements, the calculated HOMO-LUMO energy levels and the electrochemical band gaps (E_g') are shown in Table 3. These data were estimated by using the oxidation (E_{ox}) and reduction (E_{red}) peak potentials. The calculations were made by using the following equations [16, 17]:

$$E_{HOMO} = -(4.39 + E_{ox}) \quad (2)$$

$$E_{LUMO} = -(4.39 + E_{red}) \quad (3)$$

$$E_g' = E_{LUMO} - E_{HOMO} \quad (4)$$

The calculated electrochemical band gaps harmony with the optical band gap values. However, it was observed that HOMO energy levels of the polymers are lower than those of the Schiff bases. The electrochemical band gaps of polymers changed the following order: PHMP<PDEAHP<PHN< PHBD<PHB. The electrochemical band gaps values and optical band gap values support substantially each others.

Fluorescence Characteristics

The Fluorescence measurements of PDEAHP and PHB were made in different concentrations to determine the optimal concentrations in DMF. The effect of the concentration on the

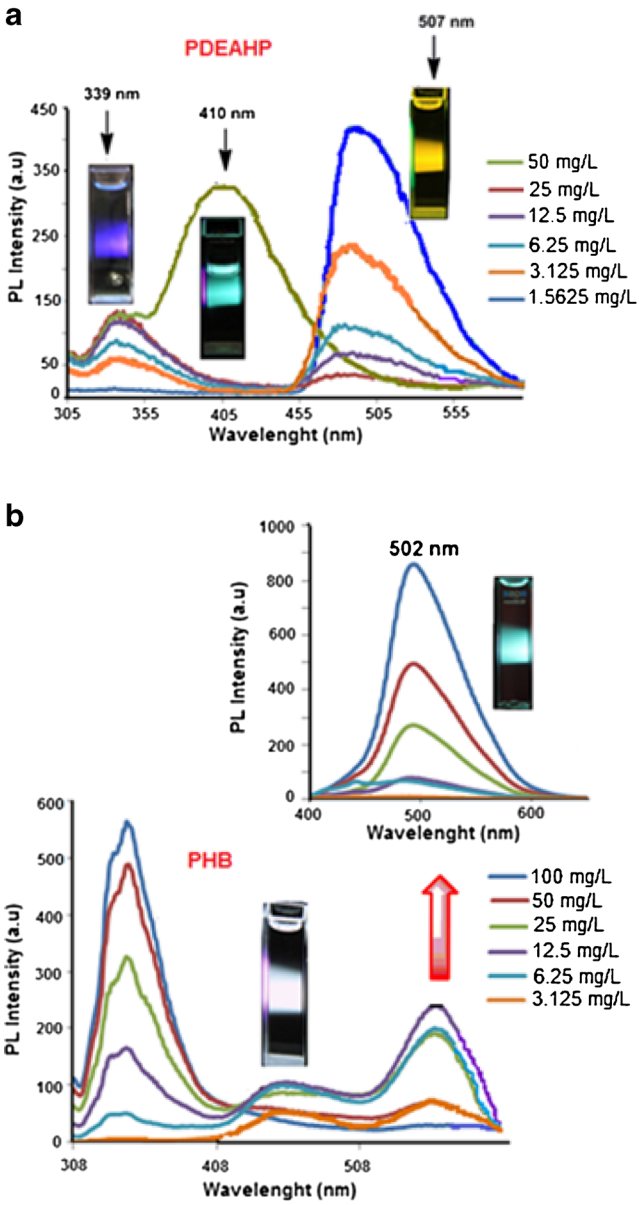

Fig. 4 Fluorescence spectra of PDEAHP (**a**), PHB (**b**) ($\lambda_{Ex.}$=277 nm, Slit: Ex: 1.5, Em: 5 nm, for PEAHDP and $\lambda_{Ex.}$=292 nm, Slit: Ex: 5 nm, Em: 5 nm for PHB)

Table 4 Fluorescence spectral data of the synthesized PDEAHP and PHB polymers

	[c]$\lambda_{max(Em)1,2}$	[d]$I_{Em1,2}$
[a]PDEAHP Conc.(mg/L)		
50	410	328
25	339, 498	30, 235
12.5	339, 498	89, 119
6.25	339, 503	117, 69
3.125	339, 505	136, 35
1.5625	339, 510	420
[b]PHB Conc.(mg/L)		
100	346	595
50	346, 556	487, 70
25	346, 558	328, 190
12.5	346, 560	164, 242
6.25	346, 560	48, 202
3.125	560	72

[a] Excitation and emission wavelengths for emission and excitation, respectively, $\lambda_{Ex.}$=277 nm and $\lambda_{Em.}$=305 nm for PDEAHP

[b] Excitation and emission wavelengths for emission and excitation, respectively, $\lambda_{Ex.}$=292 nm and $\lambda_{Em.}$=308 nm for PHB

[c] Maximum emission wavelength

[d] Maximum emission intensity

both intensity and wavelength of the emission spectra was shown Fig. 4. Fluorescence spectral data of the synthesized PDEAHP and PHB in the various concentrations are given in Table 4. Importantly, to be increasing of the concentrations of the PDEAHP and PHB, maximum emission intensity was observed higher at the fluorescence spectra. The emission wavelength of PDEAHP and PHB were changed from blue to red. It is important to emit white emission in certain concentrations of PHB solution. The compounds demonstration similar fluorescence bands have used for white light emitting diodes in the literature [18]. The high solution concentrations of PDEAHP and PHB light emit at peak wavelength forward from 500 nm. So that lowering the polymer concentration by addition of DMF showed that the fluorescence emission red shifted. While the increasing the concentration, the intensity of the emission band was decrease due to the self quenching of the molecules in the sorbet band for both compounds. π-stacked structure constructs which is consisting with concentration increase induced to hypochromic effect on B band. On the other hand, solution concentrations of PDEAHP and PHB made hyperchromic effect on Q band. This feature could be attributed to increasing of the intermolecular non-covalent π-π interactions among the molecules in the higher concentrations [19]. The intermolecular polymer-solvent affinity force is weaker than polymer-polymer association when polymer-polymer aggregation arises. Therefore, inter molecular $n \rightarrow \pi^*$ transition and n-p conjugation caused to increase of the emission band on Q band. In addition, the intensity of the entire band significantly increase and peak around 100 mg/L of PDEAHP and PHB.

A particularly interesting feature is the change in the band shape of the fluorescence emission. At the high and low concentration this shape is very similar to spectra shown for the PHN, PHMP and PHBD. However, for intermediate concentrations the spectra shape indicates the existent of two bands shown for PDEAHP and PHB.

Table 5 Thermal degradation values of the synthesized compounds

	TGA					DSC
Compounds	T_{on}[a]	$T_{max.}$[b]	T_{20}[c] (°C)	T_{50}[d] (°C)	% Char at 1000 °C	T_g[e]
PHBD	160	183, 283	260	311	23	101
HBD	213	250, 301	256	301	39	–
PHMP	151	180, 271	168	188	13	140
HMP	267	295	286	310	38	–
PDEAHP	296	301, 329	331		18	117
DEAHP	299	329	300	322	15	–
PHB	158	192, 272	192	178	3	148
HB	253	290	248	275	5	–
PHN	146	186, 299	211	294	20	119
HN	281	320	282	309	3	–

[a] The onset temperature

[b] Temperature of the peak maxima

[c] Temperature corresponding to 20 % weight loss

[d] Temperature corresponding to 50 % weight loss

[e] The glass transition temperature

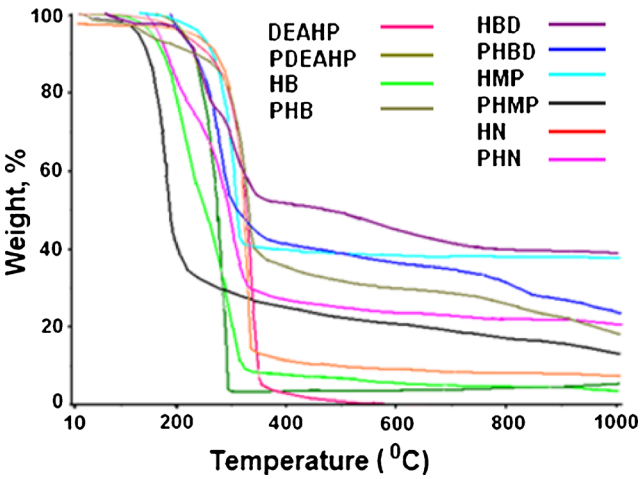

Fig. 5 TG curves of all synthesized monomers and polymers (under N_2 atmosphere at a temperature scan rate of 10 °C/min)

Florescence Quantum Yield

The fluorescence quantum yield ($Ø_F$) of the PDEAHP was measured in DMF and fluorescein was used as standard in 0.1 molar aqueous NaOH solutions. The refractive indices of the solvents were used for calculation of $Ø_F$. The new compound and the standard were excited at same wavelength (400 nm). Fluorescence quantum yield ($Ø_F$) were calculated by the comparative method (Eq. 5) [20].

$$\varnothing_F = \varnothing_F(\mathrm{Std})\frac{F.A_{Std}.n^2}{F_{Std}.A.n^2_{Std}} \quad (5)$$

Thermal Properties of Polymers

Thermal decomposition data of compounds are given in Table 5. The TGA curves of the synthesized polymers are shown in Fig. 5. According to the TGA results, polymers have decomposed in two steps. The initial degradation temperatures (T_{on}) for PHBD, PHMP, PDEAHP, PHB and PHN were found to be 160, 151, 296, 158, 146 °C, respectively. The initial degradation temperatures of polymers changed the following order: PHN<PHMP< PHB<PHBD<PDEAHP. According to these results, thermal stability of PDEAHP is higher than those of the others. This case might be attributed to presence of higher C-C couplings in PDEAHP structure which was confirmed based on ^{1}H-NMR analysis. Beside PDEAHP has the most total molecular weight. It is a fact that increasing the molecular weight gains the thermal stability. The other polymers have the thermal stability in direct proportion to total molecular weight and C-C coupling. Although PHN has the most C-C coupling, its thermal stability is so bad because of the least total molecular weight. Table 5 shows the temperatures corresponding to 20 % and 50 % weight loss of the polymers. The 20 % weight losses for PHBD, PHMP, PDEAHP, PHB and PHN were calculated as 260, 188, 331, 192 and 282 °C respectively. On the other hand, the 50 % weight losses for PHBD, PHMP, PDEAHP, PHB, PHN were calculated as 331, 188, 310, 148 and 294 °C respectively. From these results, it can be said that the synthesized polymers are thermally stable. The glass transition temperatures of polymers were determined from DSC measurements and the results are given in Table 5. The glass transition temperatures of polymers were changed between 101 and 148 °C.

SEC Analysis

SEC chromatogram results of the polymers are listed in Table 6. As seen in Table 6, the PHB and PHN had three main fractions. According to the total values, the average molecular weight of PDEAHP was found to be 51,740 g mol^{-1}. The total molecular weights of polymers were found in following order: PHN<PHB< PHMP<PHBD<PDEAHP.

Surface Morphological Properties

The scanning electron microscopy (SEM) was used to characterize the morphologies of the resulting products. Figure 6 shows SEM photographs of PDEAHP and PBH. In general, the morphologies of PDEAHP and PBH were observed like rode and wire [21, 22]. The lengths of these wires were changed between 500 and 1200 nm.

Conclusion

A series of Schiff base monomers and their corresponding polymers synthesized and their structures were confirmed by UV–vis, FT-IR, ^{1}H-NMR, ^{13}C-NMR analysis. From fluorescence analysis, it was understood that PBH emitted the white light. On the other hand PBDAH exhibited multicolor emission behavior: PBDAH emitted blue-yellow and green colors as excited at different

Table 6 The number-average molecular weight (Mn), mass-average molecular weight (Mw), polydispersity index (PDI) and % values of polymers

	Molecular weight distributions													
	Total			Fraction I				Fraction II				Fraction III			
Polymers	M_n	M_w	PDI	M_n	M_w	PDI	%	M_n	M_w	PDI	%	M_n	M_w	PDI	%
PHBD	47,500	48,280	1.02	57,100	58,200	1.02	60	33,100	33,400	1.01	40	–	–	–	–
PHMP	25,600	26,550	1.04	27,700	28,900	1.04	75	19,300	19,500	1.01	25	–	–	–	–
PDEAHP	49,690	51,740	1.04	61,650	62,300	1.01	20	46,700	49,100	1.05	80	–	–	–	–
PHB	21,055	26,025	1.20	101,000	102,500	1.01	10	17,100	23,250	1.4	40	8150	8300	1.02	50
PHN	19,300	21,400	1.11	115,800	125,250	1.01	40	37,000	39,400	1.06	15	13,600	18,500	1.05	45

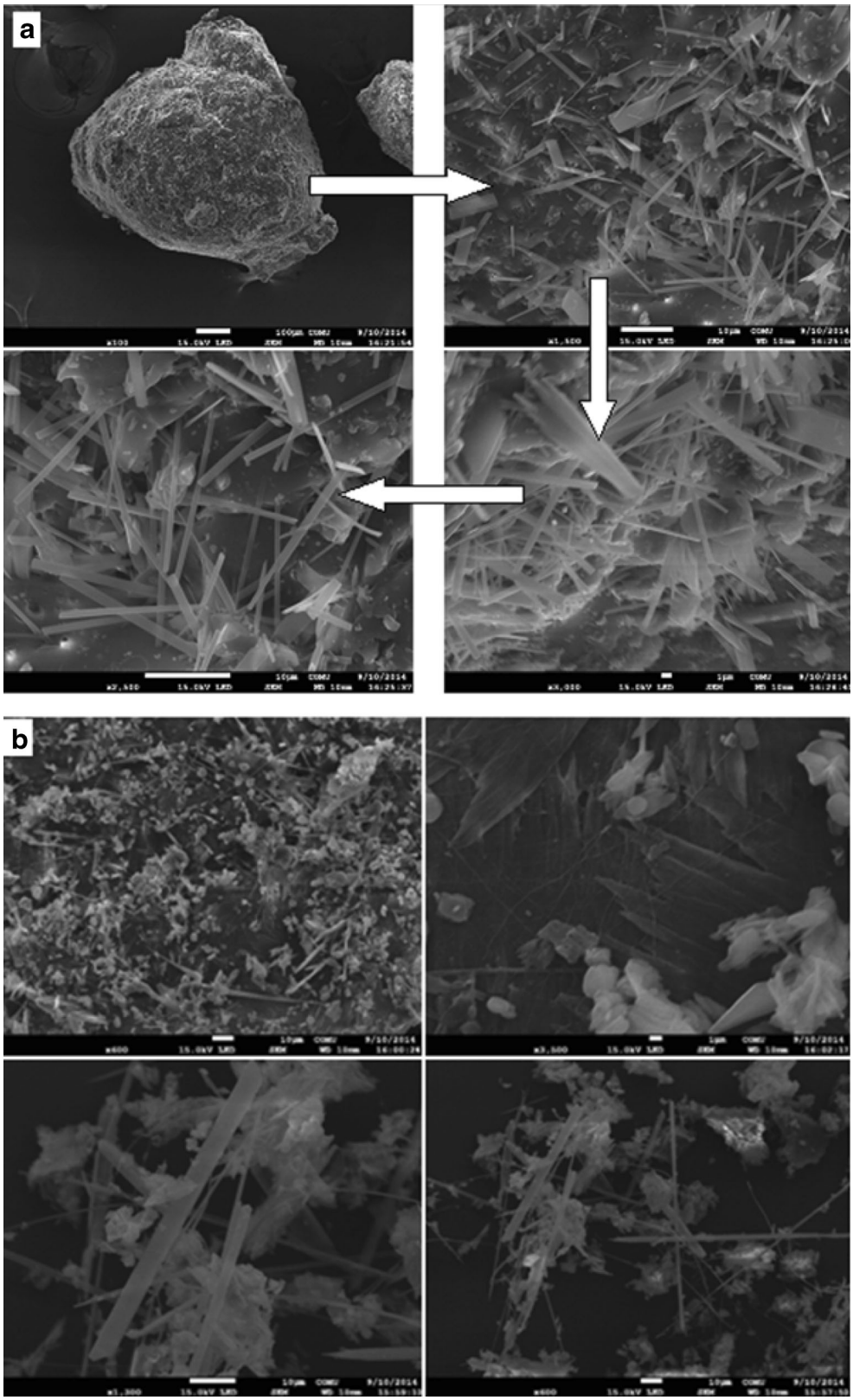

Fig. 6 SEM photographs of PDEAHP (**a**) and PHB (**b**) for different magnification with the average size of 800 nm

wavelengths. Thermal behaviors of the obtained products were evaluated by TG, DSC analysis. Fluorescence quantum yield ($Ø_F$) of PDEAHP was determined as 16 %.

References

1. Amer I, Austin D, Vosloo HCM (2003) Chemical oxidative polymerization of *m*-phenyldiamine and its derivatives using aluminum triflate as aco-catalyst. Eur Polym J 49:3251–3260
2. Selvi C, Nartop D (2012) Novel polymer anchored Cr(III) Schiff base complexes: synthesis, characterization and antimicrobial properties. Spectrochem Acta A Mol Biomol Spectrosc 95:165–171
3. Kaya İ, Vilayetoğlu AR, Mart H (2001) The synthesis, characterization and thermal stability of oligo-4-hydroxybenzaldehyde. Polym Degrad Stab 42:4859–4864
4. Kaya İ, Aydın A (2012) A new approach for synthesis of electroactive phenol based polymer: 4-(2,3-Di(thiophen-2-yl)-1H-pyrrol-1-yl)phenol and its oxidative polymer. Prog Org Coat 73: 239–249
5. Bruma M, Hamciuc E, Schulz B, Kopnick T, Kaminorz Y, Robison J (2001) New aromatic polyethers containing phenylquinoxaline and 1,3,4-oxadiazole rings. Polymer 42:5955–5961
6. Grigoras M, Catanescu CO, Macromol J (2004) Synthesis and study of arylene vinylene and aryleneimine-type polymers containing N-hexyl-3,6-carbazolyl groups. Macromol Sci C Polym Rev C44(2):1–37
7. Barbarin F, Blance JP, Dugay M, Fabre C, Maleysson C (1984) Conductivity and E.S.R. investigations of doping and dedoping in poly-Pazophenylene and poly-*p*henylene azomethine. Synth Met 10: 71–78
8. Hauer CK, King GS, McCool EL, Euler WB, Ferrara JD, Youngs WJ (1987) Structure of 2,3-butanedionedihydrazone and IR study of higher polyazines: a new class of polymeric conductors. J Am Chem Soc 109:5760–5765
9. Cheng T, Xu Y, Zhang S, Zhu W, Qian X, Duan L (2008) A highly sensitive and selective off on fluorescent sensor for cadmium in aqueous solution and living cell. J Am Chem Soc 130:16160–16161
10. Kaya İ, Kamacı M (2013) Highly selective and stable florescent sensor for Cd(II) based on poly(azomethine-urethane). J Fluoresc 23(1):115–121
11. Mirochnic AG, Bukvetskii BV, Fedorenko EF, Karasev VE (2004) Crystal structures and excimer fluorescence of anisoylbenzoylmethanatoboron and dianisoylmethanatoboron difluorides. Russ Chem Bull 53:291–296
12. Bilici A, Doğan F, Yıldırım M, Kaya İ (2013) Facile synthesis of self-stabilized polyphenol nanoparticles. Mater Chem Phys 140:66–74
13. Yıldırım M, Kaya İ (2012) Synthesis and characterization of iminothiazole bearing polyphenol with adjustable white-yellow photoluminescence color. Synth Met 162:2443–2450
14. Yıldırım M, Kaya İ (2012) A comparative study of aminothiazole-based polymers synthesized by chemical oxidative polymerization. Synth Met 162:436–443
15. Colladet K, Nicolas M, Goris L, Lutsen L, Vandezande D (2004) Low-band gap polymers for photovoltaic applications. Thin Solid Films 451:7–11
16. Cervini R, Li XC, Spencer GVC, Holmes AB, Moratti SC, Friend RH (1997) Electrochemical and optical studies of PPV derivatives and poly(aromatic oxadiazoles). Synth Met 84:359–360
17. Yıldırım M, Kaya İ (2009) Soluble semi-conductive chelat polymers containing Cr(III) in the backbone: synthesis, characterization, optical, electrochemical, and electrical properties. Polymer 50:5653–5660
18. Sakai A, Tanaka M, Ohta E, Yoshimoto Y, Mizuno K, Ikeda H (2012) White light emission from a single component system: remarkable concentration effects on the fluorescence of 1,3-diaroylmethanatoboron difluoride. Tetrahedron Lett 53:4138–4141
19. Çoşut B, Yeşilot S, Durmuş M, Kılıç A (2013) Synthesis and fluorescence properties of hexameric and octameric subphtalocyanines based cyclic phosphazenes. Dyes Pigments 98:442–449
20. Frey-Forgues S, Lavabre D (1999) Are fluorescence quantum yields so tricy to measure. A demonstration using familiar stationery products. J Chem Educ 76:1260–1269
21. Wang J, Bunimovich YL, Sui G, Savvas S, Wang J, Guo Y, Heath JR, Tseng H (2006) Electrochemical fabrication of conducting polymer nanowires in an integrated microfluidic system. Chem Commun 29: 3075–3082
22. Fowler JD, Virji S, Kaner RB, Weiller BH (2009) Hydrogen detection by polyaniline nanofibers on gold and platinum electrodes. J Phys Chem C 113:6444–6449